Letters

An Implementation Method of Capacitive Power Transfer in Seawater Environments With Single-Wire Connection Using Seawater Ionic Conduction Effect

Xichen Liu, Shuai Wu, *Member, IEEE*, Chenghao Li, *Graduate Student Member, IEEE*, and Chunwei Cai, *Member, IEEE*

***Abstract*—The strong ionic conduction of seawater creates a quasielectrostatic shielding effect, leading to weak capacitive power transfer (CPT) with the mutual coupling between capacitors suppressed. To achieve undersea CPT, this letter proposes and introduces an implementation method using a single wire to connect two Y-type capacitors, thus constructing a dual-pathway system where seawater serves as second conductive channel. The single wire is designed to provide an additional conduction path for power loop, which guides current in the seawater to the receiver. The conductive principle of the method is first introduced, describing the power flow and the distribution of the displacement and conduction current. Then, a *LC-CL* compensated topology with single wire and Y-type capacitors is analyzed to obtain constant voltage output. Finally, an experimental prototype is built to verify the proposal. The results indicate the system can successfully transfer 2 kW with 91% dc-dc efficiency to the load.**

***Index Terms*—Capacitive power transfer (CPT), dual-current-path, ionic conduction, single-wire connection.**

I. Introduction

RECHARGING marine equipment, particularly in deep-sea environment, is crucial for prolonging operational durations and supporting multifunctional deployments in harsh seawater condition [1]. However, the inevitable large-scale misalignment caused by hydrodynamic disturbances hinders the application of inductive power transfer technology and corresponding mechanical device such as trumpet-shaped dock station is difficult to guarantee perfect performance in the actual ocean [2]. Also, since metal is usually selected as the pressure shell material of marine equipment, the influence of shell needs to be considered [3]. As an alternative option, capacitive power transfer (CPT) technology is considered to be a practical solution, since it exhibits good antioffset ability with special structure in seawater [4].

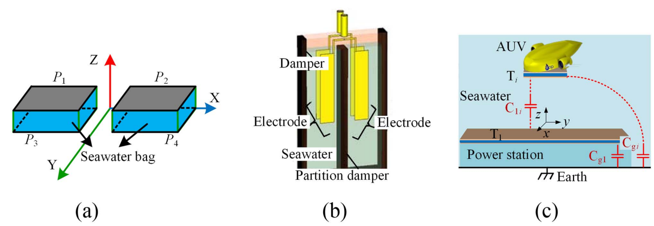

Fig. 1. (a) Seawater coupling capacitors in [7]. (b) Capacitive coupler with partition damper in [9]. (c) Schematic modeling of coupler in [10].

The main technical obstacle to implement CPT system on the marine equipment is the seawater environment, which works as ionic solution with high conductivity of 3–6 S/m varied by depth, salinity, and temperature [5]. Compared to air, seawater has a certain conductivity, but far weaker than the metal conductor. This not only puts forward requirements for insulation, but also leads to the phenomenon of strong self-coupling, which results in hard power transmission of capacitive coupler under tradition high-frequency excitation [6]. Further, the self-coupling is caused by electric field suppression, similar to electrostatic shielding.

In order to overcome this problem, recently, some research efforts have been paid on the construction of seawater capacitive power transfer (SCPT) system. In [7], two seawater bags are added in the middle of four metal plates, shown in Fig. 1(a), to model seawater condition. At this time, the ipsilateral plates are coupled by air to avoid strong self-coupling in seawater. So, the power is successfully transmitted. Similarly, Mahdi et al. [8] separated adjacent plates into different water tanks to neglect coupling effect, realizing power transmission. Then, a conductive coupler with partition damper is proposed to reduce self-coupling, as shown in Fig. 1(b). It can be pointed that the damper works as a low conductance in the equivalent circuit to block the self-coupling path. Therefore, the current is forced to

Received 5 June 2025; revised 6 August 2025; accepted 1 September 2025. Date of publication 4 September 2025; date of current version 13 November 2025. This work was supported in part by the Taishan Scholars of Shandong Province under Grant tsqnz20240801, in part by the National Natural Science Foundation of China under Grant 52571379, and in part by the Major Scientific and Technological Innovation Project of Shandong Province of China under Grant 2022ZLGX04. *(Corresponding author: Chunwei Cai.)*

The authors are with the School of New Energy, Harbin Institute of Technology-Weihai, Weihai 264209, China, and also with Key Laboratory of Cross-Domain Synergy and Comprehensive Support for Unmanned Marine Systems, Ministry of Industry and Information Technology, Weihai 264209, China (e-mail: 21s030155@hit.stu.edu.cn; wushuai@hit.edu.cn; 23b906007@stu.hit.edu.cn; caichunwei@hit.edu.cn).

Color versions of one or more figures in this article are available at https://doi.org/10.1109/TPEL.2025.3605952.

Digital Object Identifier 10.1109/TPEL.2025.3605952

flow to the receiving side, achieving large power transmission with stable transfer efficiency in a wide range [9]. The above methods all show good performance and can be classified as mechanical isolation. Unfortunately, since the seawater is hard to control in the actual ocean environment and partially works as conductor, there are two main limits in the application: 1) High installation difficulty; and 2) potential coupling between separated seawater.

For addressing these limits, Da et al. [10] proposed an underwater single capacitive coupled wireless power transfer system in submerged environment, utilizing the parasitic capacitance of metal plates, inverter, and rectifier to ground or infinity to form a virtual branch, as illustrated in Fig. 1(c). It constitutes a closed electrical loop with coupled capacitance between metal plates and then achieves 200 W power transfer with well misalignment tolerance. However, considering the seawater is connected to the ground and exhibits quasielectrostatic shielding effect, the electric field is restrained by seawater near the plate. That is, the stray capacitance is shielded by seawater, which is different from the case in air and remains the strong self-coupling phenomenon. So, there is not a strong enough electric field transmitted form transmitter to earth, and then back to receiver for supporting power flow.

The abovementioned studies have explored different methods to achieve power transfer in conductive seawater environment, giving valuable inspirations. Therefore, the authors also have carried out the relevant research in [4], modeling the seawater capacitive coupler and analyzing the power transmission ability based on the conduction path of seawater. In addition, a simple system is used to achieve power transmission for verifying the theory. But the detailed implementation method and working principle are lacked. So, for further promoting the adaptability of CPT system in the actual ocean, overcoming the installation difficulty and quasielectrostatic shield effect, this letter proposes an undersea CPT implementation method using single wire and seawater ionic conduction effect and introduces its working principle from the perspective of micro and circuit.

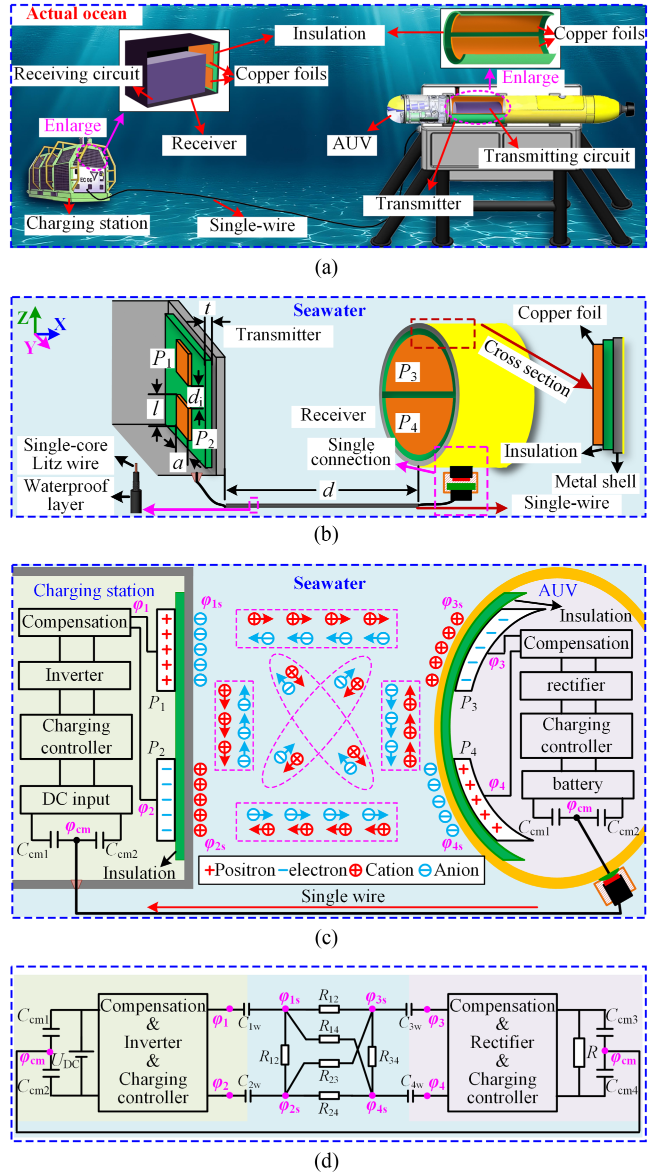

Fig. 2. (a) General overview of the proposed CPT system with single wire and Y-type capacitors. (b) diagram of the seawater capacitive coupler and single-wire. (c) Conductive principle of the proposed system. (d) Circuit diagram of the proposed system.

II. Analysis of CPT System With Single-Wire

A. Overall Configurations of the Proposed System

Facing the ionic solution of seawater with quasielectrostatic shielding effect, the general overview of the proposed method with single wire connection between two Y-type capacitors is depicted in Fig. 2(a). As shown in Fig. 2(b), two copper foils P_3 and P_4 are attached to the inner wall in an arc shape to adapt the original structure of the autonomous underwater vehicle (AUV) on the receiving side. And an insulation is added between them considering the material of AUV shell is usually made of metal to withstand pressure. It should be noted that the AUV shell and seawater can be regarded to be electrical connected under high frequency excitation due to the large contact area and high conductivity of seawater. The circuit including Y-type capacitors is later placed inside the cabin. On the transmitting side, the copper foils P_1 and P_2 and circuit are similarly installed. At this time, the transmission distance d is defined as the length between transmitter and receiver, equal to the length of single-wire. As for the single wire, which consists of waterproof layer and a single-core Litz wire because of high-frequency current flowing, it is extracted from the charging station and AUV through the preset watertight interface, respectively. Since the electric field is shielded by seawater, a real conductive path is the key to construct the power loop of undersea CPT system. The Y-type capacitors are designed for ensuring electric safe considering cable rupture.

At this time, the electron of metal plate is guided to gather on the surface, forming displacement current in the insulation. And then, the ion in seawater is driven to generate conduction current, depicted in Fig. 2(c). Hence, the circuit diagram based on single wire connection between two Y-type capacitors can be described as Fig. 2(d). The conductive principle will be introduced below.

Of course, the existence of single wire limits the convenience of the system compared to wireless power transfer system, but it enjoys the following merits based on the limited application of them:

1) Breaking through the mechanical isolation and the virtual branch of CPT system applied in actual ocean applications, implementing effective undersea CPT;
2) Eliminating one wire compared to wet-mate technology, reducing implementation difficulty of sealing design since only single-core cable needs to be connected underwater, tolerating seawater intrusion without risk of short-circuit;
3) Possessing good concealment considering there is almost no electromagnetic leakage based on two conductive paths of seawater and single wire and no seawater electrolysis occurring since power is transmitted to seawater through the coupling capacitance in insulation.

B. *Conductive Principle for Power Transmission*

As illustrated in Fig. 2(c), the presence of the insulation layer serves to isolate the copper foil electrode from the ions in seawater, thereby creating a coupling capacitance which ensures that power transmission remains a purely electrical phenomenon. At this time, based on the zero potential of the negative electrode of the dc input, a common potential φ_{cm} is established between transmitter and receiver by the single wire. Therefore, the metal plates P_{i} (i = 1,2,3,4) will be given a potential φ_{i} separately through compensation when the system works. The plate P_1 is firstly taken as an example to describe principle. In the positive half cycle, the electrons in P_1 are driven to the other plate P_2 by the relative potential. And then the aggregated positron will attract the anions in seawater to accumulate at the solid-liquid interface, causing a potential $\varphi_{1\mathrm{s}}$. Similarly, $\varphi_{2\mathrm{s}}$, $\varphi_{3\mathrm{s}}$, and $\varphi_{4\mathrm{s}}$ are obtained. So, the connection between transmitter and receiver is established and the main capacitive coupling exists in the insulation due to accumulation of charge. Basing on the ion conduction of seawater, the cations and anions in the ocean will start to move directionally at the speed of light reaction driven by different potential φ_{is}, forming six conduction currents. It is worth noting that since the movement speed of ions is mm/s, neither cations nor anions move much distance. In addition, the conduction path is diverse when the system is immersed into seawater. Both of them lead to low conductive loss in seawater similar to the earth resistance, mainly depending by the contact area. In negative half cycle, the potential is reversed, then the direction of the carriers in seawater is changed, ensuring stable operation.

Furthermore, as shown in Fig. 2(d), the circuit diagram of the proposed system on basis of the physical meaning is given for a clear explanation. Among them, the capacitors $C_{1\mathrm{w}}$, $C_{2\mathrm{w}}$, $C_{3\mathrm{w}}$, and $C_{4\mathrm{w}}$ represent the quasielectric double layer capacitances, which are formed by electron and ion adsorption. At this time, through displacement current of the insulation, the power is transmitted to the seawater without contact. As for resistances R_{12}, R_{13}, R_{14}, R_{23}, R_{24}, and R_{34}, they represent six conduction paths of seawater, which are formed by the loss caused by directional movement of ions. Considering the seawater resistance is low to exhibit strong self-coupling, leading to weak power transfer. It can be pointed that the potential φ_3 and φ_4, generated by the common potential φ_{cm}, are the key to transfer power to the load. As for the Y-type capacitors, they are designed according to the practical application for avoiding the direct connection between the source and load. Also, their symmetric design reduces the complexity of analysis in the following section.

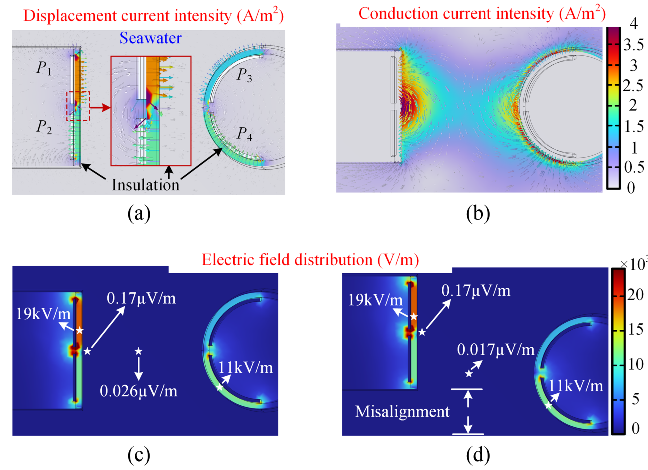

Fig. 3. (a) Displacement current intensity. (b) Conduction current intensity. (c) Electric field distribution when aligned. (d) Electric field distribution when misalignment occurs.

A vital consideration in the design of CPT system with single wire is that seawater works as conductor, resulting in nearly no displacement current in seawater to support wireless power transmission. To investigate the displacement and conduction current distribution of the given system, 500 W simulations based on COMSOL are conducted in this letter. Fig. 3(a) shows that the displacement current mainly exists in the insulation and partially exists in the charging station and cabin by air. It is hard to observe it in seawater, agreeing well with the phenomenon of the quasielectrostatic shielding. For the conduction current, shown in Fig. 3(b), there are different flow directions and the central region is weaker because of relative long transfer distance. Meanwhile, the electric field distribution is tested depicted in Fig. 3(c) and Fig. 3(d). It can be pointed out that the electric field distribution is almost unchanged, indicating independent of distance. And there are only 0.026 μV/m and 0.017 μV/m of electric field strength existing in seawater, which means low conduction loss. Hence, a small part of the seawater area can be regarded as equipotential body in special conditions.

C. *Coupling Capacitance of the Seawater Capacitive Coupler Under Finite Element Simulation*

On basis of the small part of seawater surrounded around the coupler as equipotential body, a simulation model of COMSOL is constructed for investigating the characteristic of coupling capacitance of the proposed method. For a comprehensive analysis, the coupling capacitance $C_{1\mathrm{w}}$, $C_{3\mathrm{w}}$, and C_{13} are selected to be

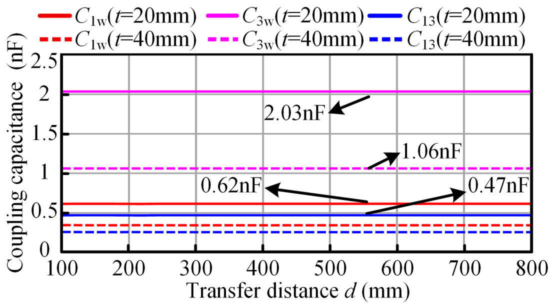

Fig. 4. Coupling capacitance varied with transfer distance under different thickness of insulation.

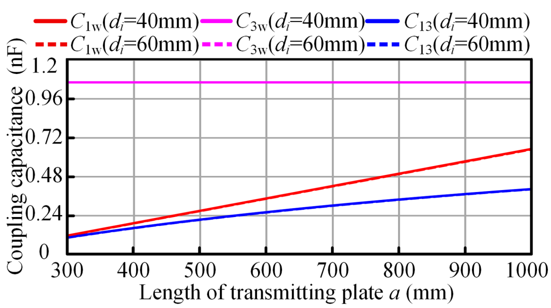

Fig. 5. Coupling capacitance varied with the length of transmitting plate under different ipsilateral distance.

measured different conditions based on symmetrical structure. Here, C_{13} is the result of measurement from P_1 and P3 when P_2 and P_4 are disconnected. When the transfer distance d varies under different thickness of the insulation t, the results are shown in Fig. 4. It can be pointed out that the coupling capacitance is hardly affected by the transfer distance and its value is approximately proportional to the thickness of the insulation, such as 1.06 nF(t = 40 mm) to 2.03 nF (t = 20 mm) of C_{3w}. The deviation can be attributed the additional coupling capacitance with ipsilateral plates and metal shell without insulation. Also, the value of C_{13} is equal to the calculated value of (1), which can be derived from the simplified circuit in Fig. 2(d) as follows:

$$C_{13} = \frac{C_{1w} * C_{3w}}{C_{1w} + C_{3w}}. \tag{1}$$

For further discussing the capacitive coupling of coupler in seawater, the impact of plate size a and ipsilateral distance d_i for the coupling capacitance is also tested and illustrated in Fig. 5. It is noticed that the ipsilateral distance only changes in the transmitting side for reducing the complexity of analysis. The results can be seen that the coupling capacitance C_{1w} increase with the length of the transmitting plate and C_{3w} is constant, indicating the capacitive coupling in the transmitter and receiver in seawater does not affect each other. In addition, the ipsilateral distance has less influence on the coupling capacitance, shown as the coincident curve. These phenomena are the particularities of seawater capacitive coupler and also the reason for its strong antidislocation ability since main capacitive coupling exists in the insulation.

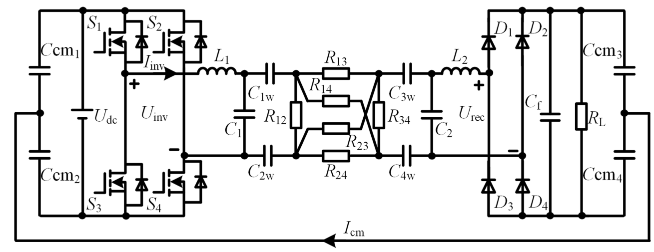

Fig. 6. Schematic of seawater CPT system circuit with single wire and Y-type capacitors.

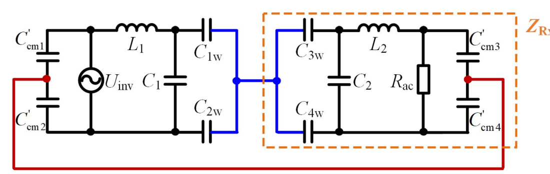

Fig. 7. Simplified circuit of the proposed undersea CPT system circuit.

III. System Circuit Topology Analysis

In this section, a dual LC compensation topology is used to enhance the power transmission capability and the new circuit structure with single wire and Y-type capacitors is analyzed later. The proposed seawater CPT system circuit is depicted in Fig. 6. It shows that a dc source U_{dc}, inverter, compensated inductors $L_1(L_2)$, compensated capacitors $C_1(C_2)$, rectifier, and load R_L form the traditional CPT system power channel. Except them, four identical capacitors C_{cmi}, single wire, and the special circuit model of four plates, which consists of four coupling capacitors C_{iw} and six resistors R_{ij} (j = 2,3,4), all lead to the different circuit characteristics and realize power transmission. Hence, the operating condition and output performance of the system under angular frequency ω are deduced below.

Based on additional single wire connection, the whole circuit structure is changed and causes an unbalanced input and output current of the inverter and rectifier, satisfying as (2). For the inverter, the impact is small except for the increase in loss since it works in the full turn-ON state. But for rectifier, the condition is different. The deviated current of rectifier will cause the diodes of the same bridge arm conducting, such as D_1 and D_2 ON. This will lead to a dead zone of input voltage of the rectifier, deteriorating system performance. At this time, the circuit works in multiple modes, which greatly increases the complexity of analysis. But the phenomenon can be suppressed by reducing the value of current in single wire I_{cm}. So, the following analysis ignores the unbalanced phenomenon and the further research will be studied for it in the future.

$$I_{inv1} = I_{inv2} + I_{cm}, I_{rec1} = I_{rec2} + I_{cm}. \tag{2}$$

Since the LC resonant network works as a band-pass filter, the fundamental mode analysis can be utilized to establish the simplified circuit, shown in Fig. 7. Among them, the seawater resistors are ignored due to the low voltage drop. In addition, the fundamental rms of the output voltage of the inverter U_{inv}, load resistance R_{ac}, and Y-type capacitance C_{cm} are obtained

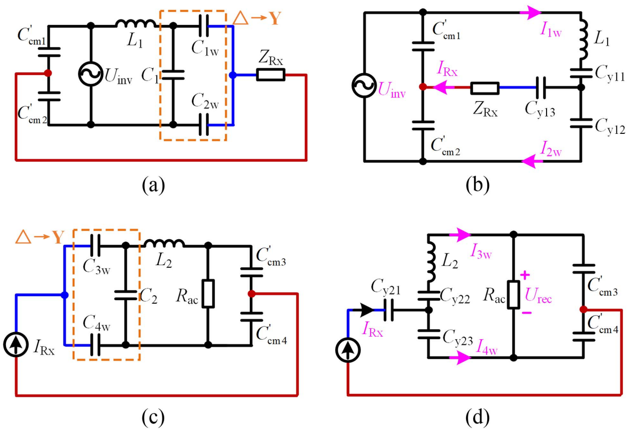

Fig. 8. (a) Equivalent circuit of transmitting side. (b) Simplified circuit of (a). (c) Equivalent circuit of receiving side. (d) Simplified circuit of (c).

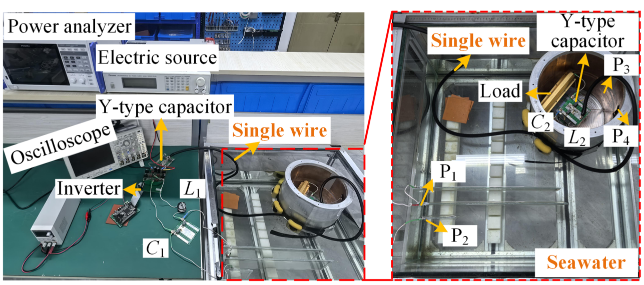

Fig. 9. Prototype of the proposed sweater CPT system with single wire.

as follows:

$$U_{\text{inv}} = \frac{2\sqrt{2}}{\pi}U_{\text{dc}}, R_{\text{ac}} = \frac{8}{\pi^2}R_{\text{L}}, C'_{\text{cm}} = C_{\text{cm}}. \tag{3}$$

At this time, the red line and blue line of the circuit represent the two conduction paths of single wire and seawater, forming a power loop. Then, the receiver can be equal to the impedance Z_{Rx} and the equivalent circuit is illustrated as Fig. 8(a).

Furthermore, by star delta changeover, Fig. 8(a) is simplified as Fig. 8(b), in which the C_{y11}, C_{y12}, and C_{y13} are given as follows:

$$\begin{cases} C_{\text{y11}} = \frac{C_1C_{1\text{w}} + C_1C_{2\text{w}} + C_{1\text{w}}C_{2\text{w}}}{C_{2\text{w}}} \\ C_{\text{y12}} = \frac{C_1C_{1\text{w}} + C_1C_{2\text{w}} + C_{1\text{w}}C_{2\text{w}}}{C_{1\text{w}}} \\ C_{\text{y13}} = \frac{C_1C_{1\text{w}} + C_1C_{2\text{w}} + C_{1\text{w}}C_{2\text{w}}}{C_1} \end{cases} \tag{4}$$

The KVL and KCL equations of Fig. 8(b) can be described As follows:

$$\begin{cases} U_{\text{inv}} = I_{1\text{w}}(j\omega L_1 + 1/j\omega C_{\text{y11}}) + I_{2\text{w}} * 1/j\omega C_{\text{y12}} \\ I_{\text{Rx}} = I_{1\text{w}} - I_{2\text{w}} \end{cases}. \tag{5}$$

It can be pointed that the output current I_{Rx} will be constant according to (6) when the relationship is satisfied as follows:

$$I_{\text{Rx}} = -j\omega U_{\text{inv}}(C_1C_{1\text{w}} + C_1C_{2\text{w}} + C_{1\text{w}}C_{2\text{w}})/C_{1\text{w}} \tag{6}$$

$$j\omega L_1 + 1/j\omega C_{\text{y11}} = -1/j\omega C_{\text{y12}}. \tag{7}$$

TABLE I
PARAMETERS OF SEAWATER CPT PROTOTYPE

Parameters	Value	Parameters	Value	Parameters	Value
U_{DC}	200 V	R_{L}	15 Ω	f	300 kHz
$C_{1\text{w}}$	22 nF	$C_{2\text{w}}$	1.68 nF	$C_{3\text{w}}$	21.9 nF
R_{c1w}	1.14 Ω	R_{c2w}	3.6 Ω	R_{c3w}	1.95 Ω
$C_{4\text{w}}$	1.51 nF	L_1	24.34 μH	L_2	24.66 μH
R_{c4w}	5.13 Ω	R_{L1}	0.15 Ω	R_{L1}	0.15 Ω
C_1	10 nF	C_2	10 nF	C_{cm}	20 nF

Combined with (4), the resonant condition is derived as follows:

$$L_1 = 1/\omega^2/(C_1 + C_{1\text{w}}C_{2\text{w}}/(C_{1\text{w}} + C_{2\text{w}})). \tag{8}$$

As for the receiving side, similar analysis is performed and the resonant relationship and output voltage are deduced in (9) and (10). At this time, the stable system output is finally achieved and the Y-type capacitors have no effect on it but keep safe in case of cable rupturing underwater, avoiding the short-circuit of the power source through the seawater.

$$L_2 = 1/\omega^2/(C_2 + C_{3\text{w}}C_{4\text{w}}/(C_{3\text{w}} + C_{4\text{w}})) \tag{9}$$

$$U_{\text{rec}} = -U_{\text{inv}}\frac{C_{3\text{w}}(C_1C_{1\text{w}} + C_1C_{2\text{w}} + C_{1\text{w}}C_{2\text{w}})}{C_{1\text{w}}(C_2C_{3\text{w}} + C_2C_{4\text{w}} + C_{3\text{w}}C_{4\text{w}})}. \tag{10}$$

IV. EXPERIMENTAL VERIFICATION

A. Experimental Prototype

For verifying the proposal and previous analysis, a practical prototype is built, as shown in Fig. 9. Two different aluminum plates covered by soda lime glass are utilized as transmitter and two copper foils attached to the metal shell by the silicone pad are utilized as receiver, respectively. All of them are placed in the pool, which is filled of seawater salvaged from ocean. Also, the single-wire is partially located in the seawater and receiving circuit is installed into shell. Then, their coupling capacitance is measured by impedance analyzer and the designed parameters are listed in Table I. Among them, the turns number of compensated inductor is 12 with the core of manganese zinc ferrite PC40 and 0.05 × 1200 of Litz wire. Also, the polypropylene film capacitor MMKP82103J1000 is used as compensated capacitor with high tolerance of voltage. Besides, the SiC MOSFET IMZ120R030M1H and the Schottky diode PFR60L300PT are used for inverter and rectifier, respectively. The working frequency is chosen at 300 kHz since high coupling capacitance.

B. System Performance

The experimental waveforms are measured in Fig. 10(a). It can be seen that the output voltage of inverter U_{inv} and input voltage of rectifier U_{rec} are in reversed phase, consistent with the analysis and achieving power transfer. In addition, the input voltage of rectifier U_{rec} has a dead zone for a period of time because the unbalanced input current of the rectifier, as mentioned above. Meanwhile, the waveform of current in single wire I_{cm} is not a standard sine wave, which contains multiple harmonics

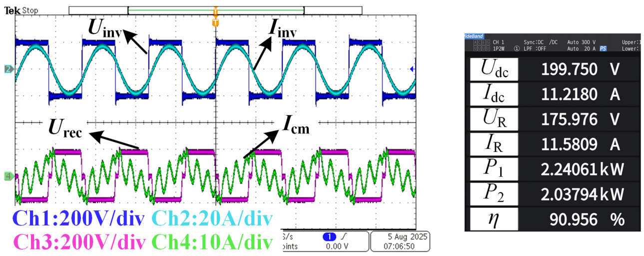

(a) (b)

Fig. 10. (a) Measured waveforms of the system. (b) Power transfer ability.

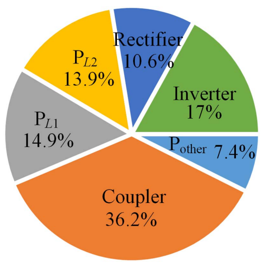

Fig. 11. Power loss distribution of the established experimental prototype.

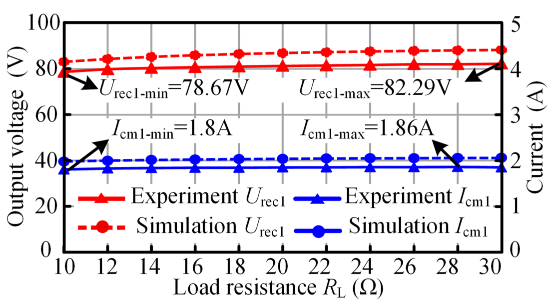

Fig. 12. Fundamental wave of system performance under varied load resistance.

with high amplitude leading to distortion. That can be attributed to the capacitance path of the system circuit such as C_{cm1}, C_{cm4}, C_{4w}, and C_{2w} under the high-order harmonics in rectangular waves of inverter output voltage. It should be emphasized that in system parameter design, the parasitic inductance of single wire should be avoided to resonate with the capacitance path under the odd harmonics of U_{inv}, resulting in a large current.

Then, the system power transfer ability is tested in Fig. 10(b). It shows that the output power reaches 2 kW with a dc-to-dc efficiency of 91%. Based on the components' inner resistance and remaining loss is assumed as other, the approximate system power loss distribution is shown in Fig. 11 due to the existence of waveforms distortion.

Furthermore, the amplitude of the fundamental wave of U_{rec1} and I_{cm1} in experiment and circuit simulation under varied load resistance is depicted in Fig. 12. At this time, the input voltage is 100 V considering the limit of electric load voltage. It exhibits good stable output performance, since the influence of dead zone is shielded by fast Fourier transformation. Meanwhile, it can be pointed out that the results of experiment and simulation is similar, verifying the previous analysis. The deviation may be caused by the influence of inverter, rectifier, and experiment accuracy as they are ideal in the simulation.

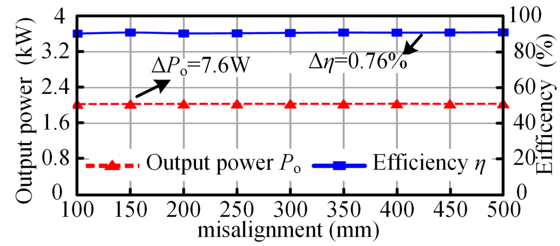

Fig. 13. System performance of power transfer and efficiency with misalignment.

TABLE II
COMPARISONS OF THE EXISTING WORKS WITH THIS LETTER

References	[7]	[9]	[10]	This letter
Power	100 W	1 kW	200 W	2 kW
Efficiency	80.15%	94.5%	71.3%	91%
Frequency	625 kHz	6.78 MHz	200 kHz	300 kHz
Physical means	Sewater bag	Partition damper	Common ground of instruments	Single wire
Potential of transfer distance	★	★	★	★★
Misalignment tolerance	★	★★	★★★	★★★
Difficulty of implementation	★	★	★	★★

The more the number of "★", the better the performance.

To verify the working principle of the proposed system based on displacement current in insulation and conduction current in seawater and single wire, the output power P_o and system efficiency η against misalignment are tested in Fig. 13. It can be seen that the maximum fluctuation of P_0 and η are only 7.6 W and 0.76%, showing almost independent of the relative location.

C. Comparison With the Existing Works

To highlight the advantages of the proposal, the current works are compared and analyzed in terms of power and efficiency, frequency, physical means, potential of transfer distance, difficulty of implementation and misalignment tolerance in Table II. It can be seen that the proposed method in seawater has certain advantages in potential of transfer distance, difficulty of implementation, and misalignment tolerance. In addition, 2 kW power transmission with the efficiency of 91% under 300 kHz is advanced compared to the existing works. In conclusion, the proposed method can promote the development of marine equipment supply.

V. CONCLUSION

This article presents an undersea CPT implementation method. The key innovation is using a single wire to create a common potential reference, forming a dual-current-path circuit with the ion conduction channel of seawater. Then, the principle of the proposed method is introduced in detail in the perspective of micro and circuit. This approach effectively circumvents seawater's quasielectrostatic shielding, enabling efficient power transfer for marine devices. The distribution of the conduction current and displacement current is then simulated, verifying the analysis. Besides, the characteristic of coupling capacitance of the coupler is tested with the variation of system parameters. For further, an *LC-CL* compensated topology is adjusted and analyzed to obtain constant voltage output under resonant frequency based on single wire and Y-type capacitors. Finally, a 2 kW prototype is established with the efficiency of 91% to verify the theoretical analysis. The experiment results show that the proposal is flexible for marine charging occasion.

REFERENCES

[1] C. R. Teeneti, T. T. Truscott, D. N. Beal, and Z. Pantic, "Review of wireless charging systems for autonomous underwater vehicles," *IEEE J. Ocean. Eng.*, vol. 46, no. 1, pp. 68–87, Jan. 2021.

[2] S. Wu, C. Cai, A. Wang, Z. Qin, and S. Yang, "Design and implementation of a uniform power and stable efficiency wireless charging system for autonomous underwater vehicles," *IEEE Trans. Ind. Electron.*, vol. 70, no. 6, pp. 5674–5684, Jun. 2023.

[3] H. T. Liu and N. Li, "Reliability analysis of autonomous underwater vehicle aft pressure shell for optimal design and strength," *Ocean Eng.*, vol. 249, 2022, Art. no. 110906.

[4] X. Liu, C. Cai, S. Wu, C. Li, Q. Cui, and X. Ren, "Modeling and analysis of undersea capacitive power transfer based on conduction current in seawater," *IEEE Trans. Power Electron.*, vol. 40, no. 3, pp. 4640–4651, Mar. 2025.

[5] Z. Zheng et al., "Three-stage vertical distribution of seawater conductivity," *Sci. Rep.*, vol. 8, no. 1, 2018, Art. no. 9916.

[6] M. Tamura, K. Murai, and Y. Naka, "Design theory of a parallel-plate coupler for underwater wireless power transfer," in *Proc. IEEE Int. Symp. Radio-Freq. Integration Technol.*, 2020, pp. 211–213.

[7] L. Yang, M. Ju, and B. Zhang, "Bidirectional undersea capacitive wireless power transfer system," *IEEE Access*, vol. 7, pp. 121046–121054, 2019.

[8] H. Mahdi, B. Hoff, P. G. Ellingsen, and T. Østrem, "Conformal transformation analysis of capacitive wireless charging," *IEEE Access*, vol. 10, pp. 105621–105630, 2022.

[9] M. Tamura, K. Murai, and M. Matsumoto, "Design of conductive coupler for underwater wireless power and data transfer," *IEEE Trans. Microw. Theory Techn.*, vol. 69, no. 1, pp. 1161–1175, Jan. 2021.

[10] C. Da, F. Li, M. Nie, S. Li, C. Tao, and L. Wang, "Undersea capacitive coupled simultaneous wireless power and data transfer for multiload applications," *IEEE Trans. Power Electron.*, vol. 40, no. 1, pp. 2630–2642, Jan. 2025.